Millimeter-Wave Fin-Line Characteristics

JEFFREY B. KNORR, MEMBER, IEEE, AND PAUL M. SHAYDA, MEMBER, IEEE

Abstract—**This paper presents an analysis of the fin line. The spectral-domain technique is used to determine both wavelength and characteristic impedance. Numerical results are compared with known data for ridged waveguide slab-loaded waveguide, and slotline. Design curves are presented for practical millimeter-wave fin line structures.**

I. Introduction

IN THE PAST several years, fin line has been increasingly used as a medium for constructing millimeter wave circuits [1]–[4]. Fig. 1 shows a cross-sectional view of a fin line. The structure may be viewed as a slotline with a shield, a ridged waveguide with dielectric or a slab loaded waveguide with fins. A major attribute of the structure is its compatability with rectangular waveguide and the ease with which the fin pattern may be realized using printed circuit techniques.

In practice, when fin lines are constructed, the dielectric material is often allowed to pass through the broad wall of the shield [1]. An additional dielectric spacer may be used to provide complete dc isolation of one fin from the shield to allow biasing of solid-state devices mounted between the fins. In this case, the wall thickness is made equal to one quarter of a wavelength thereby causing an RF short circuit to appear between the fin and the inner wall of the shield. Thus, a practical fin line will have electrical characteristics similar to the idealized structure shown in Fig. 1.

Several recent papers [5]–[7] have described methods for the determination of fin line wavelength and an approximate method for calculating characteristic impedance is suggested in [1]. This paper presents an analysis of fin line using the spectral domain technique. The analysis covers both wavelength and characteristic impedance.

The paper first discusses the application of the spectral domain technique to fin line. A new matrix approach to the implementation of this method is described. Numerical results are then presented and compared with known data for ridged waveguide, slab loaded waveguide, and slotline. These comparisons establish the accuracy of the numerical results and illustrate the applicability of the method for the full range of structure parameters. It also provides perspective on the substructures which result in the various limits. Finally, several families of design curves are presented for a practical choice of fin-line parameters.

Manuscript received November 30, 1979; revised February 7, 1980. This work was supported in part by the Naval Ocean Systems Center, San Diego, CA, and in part by the Foundation Research Program, Naval Postgraduate School, Monterey, CA.

J. Knorr is with the Department of Electrical Engineering, Naval Postgraduate School, Monterey, CA 93940.

P. Shayda is with the 3D Radar Division, Surveillance System Subgroup, Naval Sea Systems Command, Washington, DC.

II. Fin-Line Analysis

The analysis of various structures using the spectral-domain technique has been discussed previously in several papers by one of the authors as well as other researchers [7]–[12]. Thus the application of the spectral-domain technique to the analysis of a fin line will be presented here in an abbreviated fashion.

The fin line supports a hybrid field. All transverse field components may be found from

$$E_z = k_c^2 \phi^e(x,y) e^{\Gamma z} \tag{1a}$$

$$H_z = k_c^2 \phi^h(x,y) e^{\Gamma z} \tag{1b}$$

where the scalar potential functions ϕ^e, ϕ^h satisfy the Helmholtz equation, and we assume lossless propagation so that $\gamma = \pm j\beta$. Further

$$k_{ci}^2 = k_i^2 - \beta^2 \tag{2}$$

with

$$k_i^2 = \omega^2 \mu_i \epsilon_i, \qquad i = 1,2,3 \tag{3}$$

for each of the three regions defined in Fig. 1. We will assume here that $\epsilon_1 = \epsilon_3 = \epsilon_0$ and $\epsilon_2 = \epsilon_0 \epsilon_r$.

The second-order partial differential equations for the unknown potentials ϕ^e, ϕ^h may be Fourier transformed with respect to x to obtain ordinary differential equations. When this is done and boundary conditions at the shield walls are applied, we obtain the solutions

$$\Phi_1^e(\alpha_n,y) = A^e(\alpha_n)\sinh\gamma_1(D+h_1-y) \tag{4a}$$

$$\Phi_2^e(\alpha_n,y) = B^e(\alpha_n)\sinh\gamma_2 y + C^e(\alpha_n)\cosh\gamma_2 y \tag{4b}$$

$$\Phi_3^e(\alpha_n,y) = D^e(\alpha_n)\sinh\gamma_3(h_2+y) \tag{4c}$$

$$\Phi_1^h(\alpha_n,y) = A^h(\alpha_n)\cosh\gamma_1(D+h_1-y) \tag{4d}$$

$$\Phi_2^h(\alpha_n,y) = B^h(\alpha_n)\sinh\gamma_2 y + C^h(\alpha_n)\cosh\gamma_2 y \tag{4e}$$

$$\Phi_3^h(\alpha_n,y) = D^h(\alpha_n)\cosh\gamma_3(h_2+y) \tag{4f}$$

where

$$\gamma_i^2 = \alpha_n^2 - k_{ci}^2 \tag{5}$$

and

$$\alpha_n = \begin{cases} n2\pi/b, & \phi^h \text{ even} \quad (6a) \\ (2n-1)\dfrac{\pi}{b}, & \phi^h \text{ odd} \quad (6b) \end{cases}$$

0018-9480/80/0700-0737$00.75 ©1980 IEEE

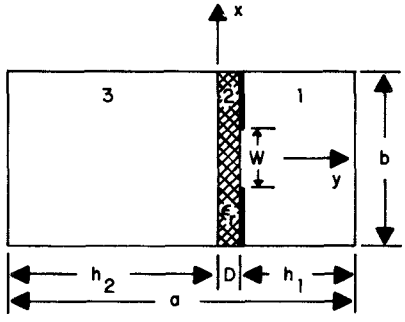

Fig. 1. Cross-sectional view of a fin line.

Through the application of boundary conditions at $y=0$ and $y=D$, the eight coefficients A^e through D^h may be related to each other, to the fin surface current, $j(x)$, and to the slot field $e(x)$. The resulting set of linear equations (really a set of transformed boundary equations) may be written in matrix form as follows:

$$[\mathfrak{M}_{\mathcal{E}}]\begin{bmatrix} A^e \\ B^e \\ \vdots \\ D^h \end{bmatrix}=\begin{bmatrix} 0 \\ 0 \\ \vdots \\ \mathcal{E}_x \\ \mathcal{E}_z \end{bmatrix} \tag{7a}$$

$$[\mathfrak{M}_{\mathcal{J}}]\begin{bmatrix} A^e \\ B^e \\ \vdots \\ D^h \end{bmatrix}=\begin{bmatrix} 0 \\ 0 \\ \vdots \\ \mathcal{J}_x \\ \mathcal{J}_z \end{bmatrix} \tag{7b}$$

where $\mathcal{E}_i(\alpha_n)$ is the transform of the slot field and $\mathcal{J}_i(\alpha_n)$ is the transform of the current. The matrices $[\mathfrak{M}_{\mathcal{E}}]$ and $[\mathfrak{M}_{\mathcal{J}}]$ differ in only the last two rows. Each is a square 8×8 matrix. Using (7a) and (7b), we may write

$$[\mathfrak{M}_{\mathcal{J}}][\mathfrak{M}_{\mathcal{E}}^{-1}]\begin{bmatrix} 0 \\ 0 \\ \vdots \\ \mathcal{E}_x \\ \mathcal{E}_z \end{bmatrix}=\begin{bmatrix} 0 \\ 0 \\ \vdots \\ \mathcal{J}_x \\ \mathcal{J}_z \end{bmatrix}. \tag{8}$$

From (8), using the four elements in the lower right-hand corner of the matrix $[\mathfrak{M}_{\mathcal{J}}][\mathfrak{M}_{\mathcal{E}}^{-1}]$, we obtain

$$[\mathcal{G}]\begin{bmatrix} \mathcal{E}_x \\ \mathcal{E}_z \end{bmatrix}=\begin{bmatrix} \mathcal{J}_x \\ \mathcal{J}_z \end{bmatrix} \tag{9}$$

where the 2×2 matrix $[\mathcal{G}]$ is the transform of the dyadic Green's function for this structure.

Previously, (9) has been obtained by extensive algebraic manipulation of the boundary equations. In the approach described here, the matrices (7) are defined directly from the boundary equations and (9) is arrived at by numerical computation. There is some sacrifice in numerical efficiency, but the formulation of the problem is more straightforward.

Equation (9) is exact, no approximations having been made so far. A solution to (9) is obtained using the Method of Moments as discussed elsewhere [7]–[12]. For this problem, we have chosen to approximate the field between the fins as

$$e_x(x)=\begin{cases} 1, & |x|\leq W/2 \\ 0, & \text{elsewhere} \end{cases} \tag{10a}$$

$$e_z=0. \tag{10b}$$

This choice has been shown to give accurate results for slotlines with $W/D\leq 2$ [11], and for dielectric-loaded waveguide, $W/b=1$, it is exact. The results to be presented shortly indicate that (10) is a good choice for the fin line as well.

The dispersion problem is now reduced to the form

$$\sum_n g_{11}(\alpha_n,\beta)|\mathcal{E}_x(\alpha_n)|^2=0. \tag{11}$$

A numerical search for the value of β which satisfies (11) yields the propagation constant for the dominant fin-line mode.

The characteristic impedance of the fin line is not uniquely defined since the field is non-TEM. A useful definition, however, is

$$Z_0=\frac{V_0^2}{2P_{\text{avg}}} \tag{12}$$

where V_0 is the voltage between the fins and P_{avg} is the time-averaged power flow. V_0, the voltage across the interface, is determined by (10a) and

$$P_{\text{avg}}=\tfrac{1}{2}\text{Re}\int_S\int(E_xH_y^*-E_yH_x^*)\,dx\,dy. \tag{13}$$

Parseval's theorem is applied to (13) to obtain

$$P_{\text{avg}}=\tfrac{1}{2}\text{Re}\frac{1}{b}\sum_{n=-\infty}^{+\infty}\int_{-h_2}^{D+h_1}[\mathcal{E}_x(\alpha_n,y)\mathcal{H}_y^*(\alpha_n,y)-\mathcal{E}_y(\alpha_n,y)\mathcal{H}_x^*(\alpha_n,y)]\,dy. \tag{14}$$

The integration with respect to y can be carried out analytically in (14). This leaves an equation of the form

$$P_{\text{avg}}=\frac{1}{2b}\sum_{n=-\infty}^{+\infty}f(\alpha_n,\beta) \tag{15}$$

which is evaluated numerically in each of the three regions.

III. Numerical Results

A computer program was developed to solve the equations presented in the previous section. To check the accuracy of the numerical results, they were compared with data available in the literature as described below.

A. Ridged Waveguide

If $\epsilon_r=1$, the fin line becomes a ridged waveguide with zero-thickness ridges. The wavelength and impedance in this case are given by

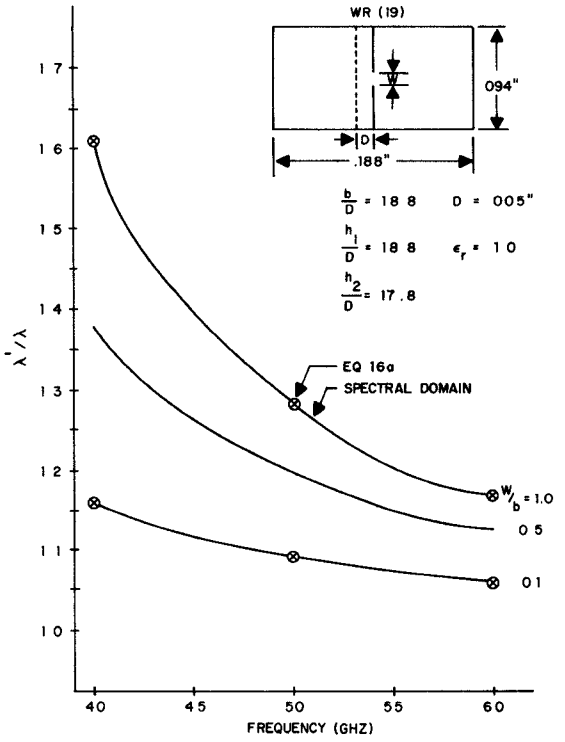

Fig. 2. Wavelength ratio λ'/λ versus frequency for a ridged waveguide. Ridges are centered and have zero thickness.

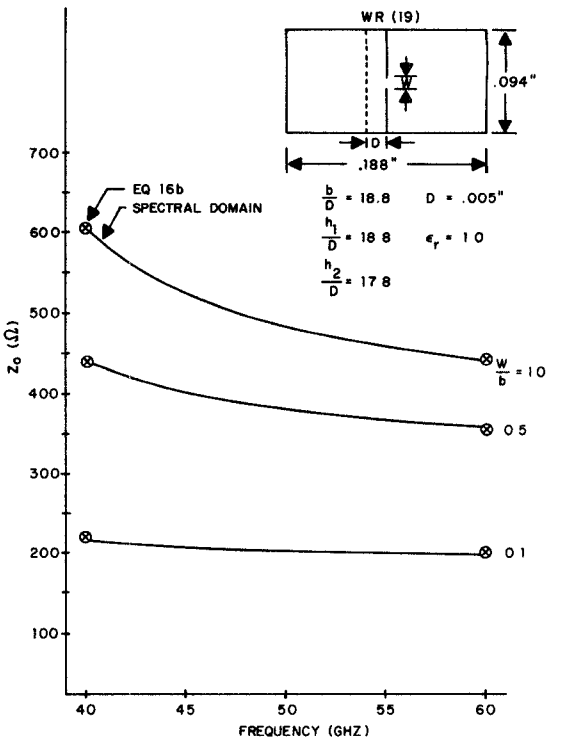

Fig. 3. Voltage impedance versus frequency for a ridged waveguide. Ridges are centered and have zero thickness.

$$\lambda'/\lambda = \frac{1}{\left[1-\left(\frac{\lambda}{\lambda_c}\right)^2\right]^{1/2}} \tag{16a}$$

$$Z_0 = \frac{Z_{0\infty}}{\left[1-\left(\frac{\lambda}{\lambda_c}\right)^2\right]^{1/2}}. \tag{16b}$$

The ridged waveguide has been treated by Hopfer [13] and Lagerlöf [14]. The cutoff wavelength λ_c was determined from [13] for several values of W/b. Equation (16a) was then used to calculate λ'/λ and these values were compared with results obtained using the spectral-domain method as shown in Fig. 2. It can be seen that the two results agree to within 0.5 percent. A similar comparison of impedance [14] as determined by both methods appears in Fig. 3. Again, the agreement is very good, with the difference being only 2 percent.

B. Slab-Loaded Waveguide

If $W/b=1$ and $\epsilon_r>1$, the fin line becomes a slab-loaded waveguide. The wavelength may easily be determined analytically by the transverse resonance procedure [15]. Fig. 4 shows the variation of λ'/λ with dielectric thickness D for several values of ϵ_r. The edge of the slab is placed at the midpoint of the broad wall of a WR(19) guide operating at 40 GHz. The agreement between the results obtained by the two methods is excellent.

The slab-loaded waveguide has also been studied by Vartanian *et al.* [16]. They consider a guide with the slab centered and give an analytical expression for the (voltage) impedance Z_{pv} (using notation of [16]) at the center of the slab. The impedance at the edge of the slab (as it is

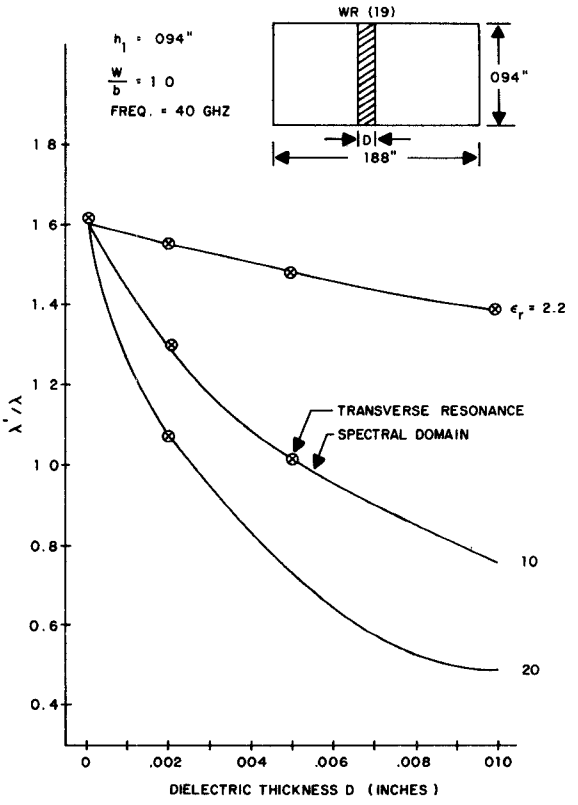

Fig. 4. Wavelength ratio λ'/λ versus dielectic thickness D for a slab-loaded WR(19) guide. Edge of slab is centered.

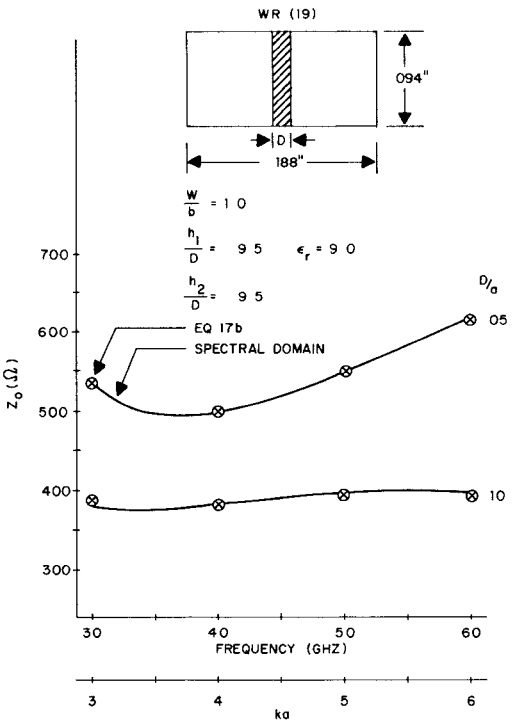

Fig. 5. Voltage impedance versus frequency for a slab-loaded WR(19) waveguide. Slab is centered.

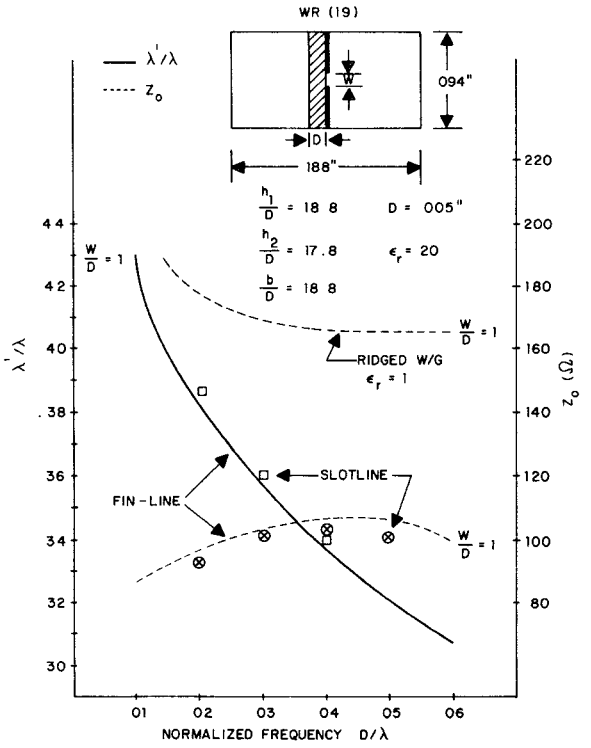

Fig. 6. Wavelength ratio λ'/λ and characteristic impedance Z_0 versus normalized frequency D/λ for a fin line and a slotline. The fin line has a WR(19) shield and fins are centered.

defined here) may easily be obtained from Z_{pv} as

$$Z_0 = Z_{pv}\left(\frac{E_x^{\text{edge}}}{E_x^{\text{ctr}}}\right)^2 \tag{17a}$$

where E_x^{edge} is the field at the edge of the slab and E_x^{ctr} is the field at the center of the slab. Thus

$$Z_0 = Z_{pv}\cos^2\frac{qc}{2s} \tag{17b}$$

where the various quantities on the right-hand side of (17b) are defined in [16]. The characteristic impedance of a slab-loaded guide was computed using both the spectral-domain method and Vartanian's equations. The results are compared in Fig. 5 where the discrete points are calculated from (17a). It can be seen that the results agree very closely.

C. Slotline

If $W/D \leqslant 2$ and D/λ and ϵ_r are sufficiently large, the field is tightly bound to the slot. For this condition, the presence of the shield will have little effect if the walls are sufficiently far removed from the slot. In this case, the fin line will behave like a slotline. This behavior is illustrated in Fig. 6 where wavelength and characteristic impedance of a fin line with $W/D = 1$, $\epsilon_r = 20$ have been plotted. The discrete points are the values of the same parameters for a slotline with equal W/D as obtained from [17]. It can be seen that the results agree closely for the two structures. The agreement is within 1 percent for wavelength and 5 percent for impedance. The impedance of the ridged-waveguide substructure has also been plotted for reference.

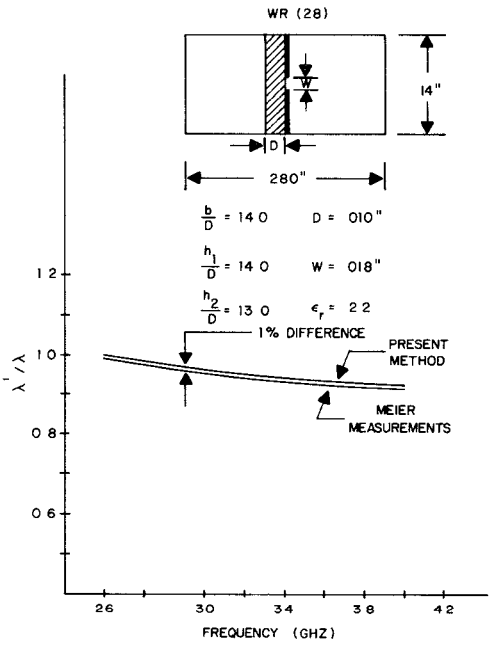

Fig. 7. Computed and measured values of wavelength ratio λ'/λ versus frequency for a fin line with WR(28) shield. Fins are centered.

D. Measurement

Fin-line wavelength measurements have been reported by Meier [1]. A computer run was made for a structure with the physical parameters reported in [1], and the results were compared with the measured values. This comparison appears in Fig. 7, where the values are seen to be in agreement to within about 1 percent.

E. Approximations

It has been suggested [1] that for low-dielectric-constant substrates the fin-line wavelength and impedance are approximated well by the relations

$$\lambda'/\lambda \doteq \frac{1}{\sqrt{k_e - \left(\frac{\lambda}{\lambda_c}\right)^2}} \tag{18a}$$

$$Z_0 \doteq \frac{Z_{0\infty}}{\sqrt{k_e - \left(\frac{\lambda}{\lambda_c}\right)^2}} \tag{18b}$$

where k_e is the effective dielectric constant and λ_c and $Z_{0\infty}$ are the cutoff wavelength and high-frequency limit impedance of the ridged-waveguide substructure. k_e is assumed invariant with frequency through the waveguide band and may be determined experimentally.

To check the accuracy of this approximation, k_e was determined for a fin line in WR(28) guide at $f=33$ GHz. This was accomplished using the numerical value of λ'/λ from Fig. 8 and the value of λ_c from [13] in (18a). The value of k_e thus determined was then assumed constant and (18) were used to calculate λ'/λ and Z_0 at $f=40$ GHz. These values were, in turn, compared with those in Fig. 8 for $W/b=0.1$, 0.5, and 1.0. Wavelength ratios agreed to within 0.2 percent while the difference in impedance values was 7–9 percent. The approximate expressions are thus useful for fin lines using low-dielectric-constant substrates. It is clear from Figs. 5 and 6, however, that there is no possibility that (18b) can be used to approximate the impedance if ϵ_r is high.

IV. Fin-Line Design Curves

In general, the publication of design curves for a structure like the fin line is problematic since there are several independently variable parameters which describe the structure. Practical considerations alleviate this difficulty to some extent, however. First, fin lines are generally enclosed with a shield that is compatible with the dimensions of the standard rectangular waveguides for the millimeter wavebands. Above 22 GHz (WR(34)), all these guides have aspect ratios $b/a=0.5$. Further, the fins are most often centered in the guide and printed using $D=$ 0.005-in substrate with $\epsilon_r=2.2$. It thus seems that it would be useful to provide design curves for structures with these parameters. This has been done for the 26.5–40-GHz, 40–60-GHz, and 60–90-GHz waveguide bands. The results appear in Figs. 8–10.

An inspection of Figs. 8–10 reveals that even with (centered) fin separations of a few mils, it is difficult to achieve low values of characteristic impedance. The lower limit for the parameters chosen here is in the range of 125–150 Ω. In some applications, it is desirable to have a lower impedance which raises the question as to how this might be achieved. One method is to increase the dielectric constant. This is clear from a comparison of Figs. 9 and 6. For a $W=0.005$-in slot, use $W/D=1$ in Fig. 6 and $W/b=0.053$ in Fig. 9 to find that the impedance is decreased from about 165 to 100 Ω when the dielectric constant is increased from $\epsilon_r=2.2$ to $\epsilon_r=20$. This approach has a disadvantage since the wavelength is decreased by a factor of 3 making already small circuit dimensions even smaller.

Another possibility for achieving a lower Z_0 might be to relocate the fins toward the sidewall of the guide. Fig. 11 illustrates the characteristics of a fin line with the fins located midway between the sidewall and the center of a WR(19) guide. Comparing Fig. 11 with Fig. 9, it can be seen that the relocation of the fins causes a small increase in the wavelength and pronounced changes in the impedance. The change in wavelength, for example, is 4 percent at 40 GHz and 2 percent at 60 GHz for $W/b=1$. The change is less for smaller values of W/b. With regard to characteristic impedance, it can be seen that the values are relatively unchanged for small values of W/b. For this situation, the line behaves like a slotline and there is little effect produced by the presence of the shield. For $W/b=1$, however, the impedance decreases significantly, from about 500 Ω for the centered configuration to about 275 Ω for the off-center configuration. In this case, the guide is also loaded, and since the low dielectric constant causes little change in the empty guide fields, the result agrees with expectations based on the voltage-impedance definition for an empty guide. The interesting feature of the results here is that the impedance for $W/b=1$ falls below that for $W/b=0.5$. Thus for the off-center configurations, the impedance first increases with W/b, then reaches a maximum, and decreases until $W/b=1$. Overall, it seems clear that relocation of the fins toward the side of the guide does not result in lower structure impedance when W/b is small. It should also be noted that the ridged waveguide data necessary for the evaluation of the approximate expressions given by (18) are not readily available in the literature.

Probably the best way to realize a lower structure impedance is to use a single-fin structure. If a single fin were separated from the bottom wall of the shield by a distance $W/2$, then for small values of W/b the impedance would be approximately one half that for a normal fin line with fin spacing W. For example, Fig. 8 shows that the impedance of a WR(28) fin line with $W/b=0.05$ ($W=0.007$ in) is approximately $Z_0=160$ Ω. Thus a single fin in the same shield would result in a structure impedance of approximately $Z_0=80$ Ω if located a distance $W=0.0035$ in from the bottom wall of the shield. This configuration has the additional advantage that the bottom wall of the shield may be used as a heat sink.

V. Conclusions

A transform method of obtaining the wavelength and characteristic impedance for the dominant mode of the fin line has been presented. It has been shown that a matrix formulation of the problem permits the elements of the

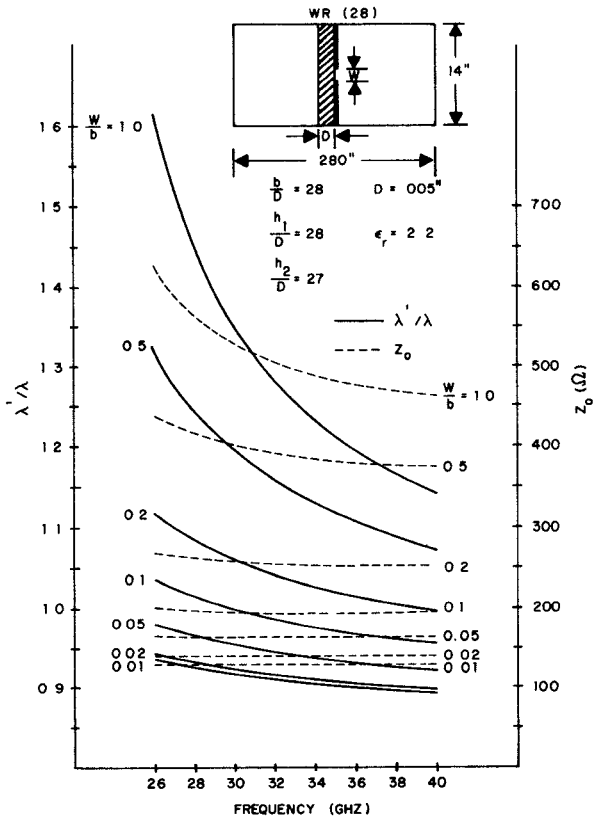

Fig. 8. Wavelength ratio λ'/λ and characteristic impedance Z_0 versus frequency for a fin line with WR(28) shield. Fins are centered.

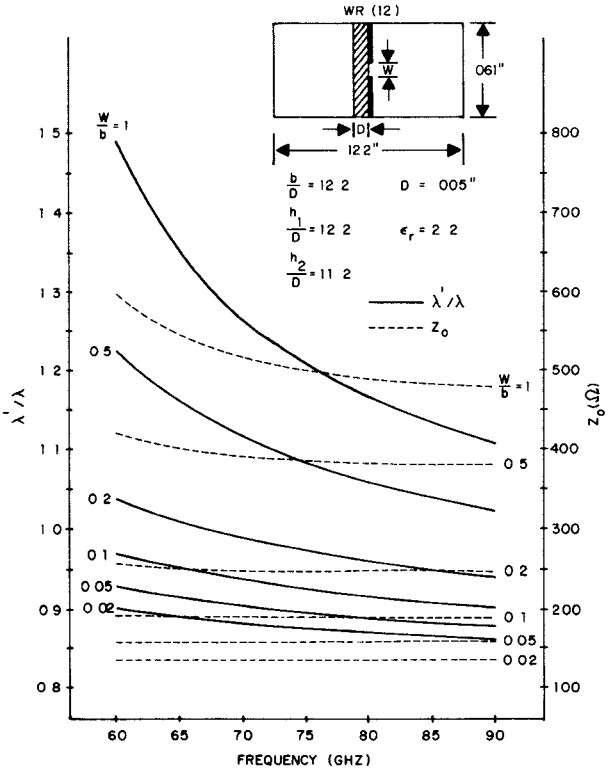

Fig. 10. Wavelength ratio λ'/λ and characteristic impedance Z_0 versus frequency for a fin line with WR(12) shield. Fins are centered.

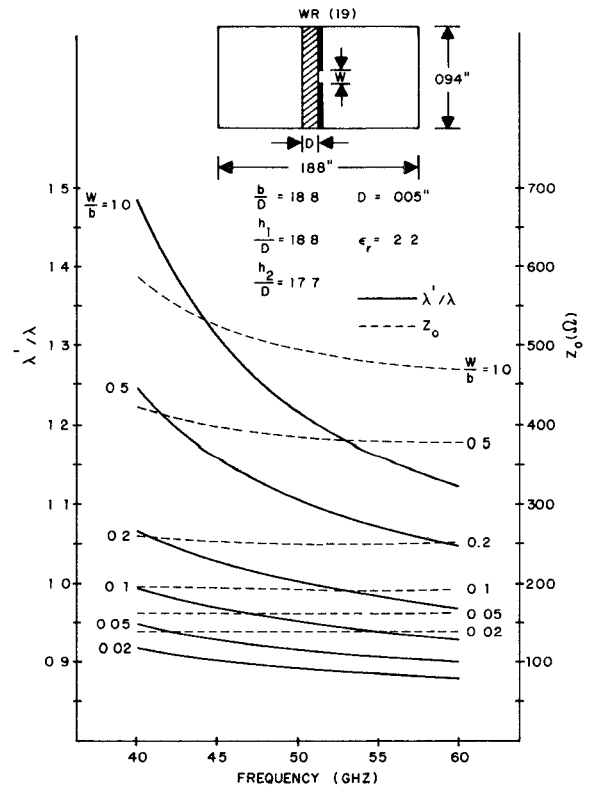

Fig. 9. Wavelength ratio λ'/λ and characteristic impedance Z_0 versus frequency for a fin line with WR(19) shield. Fins are centered.

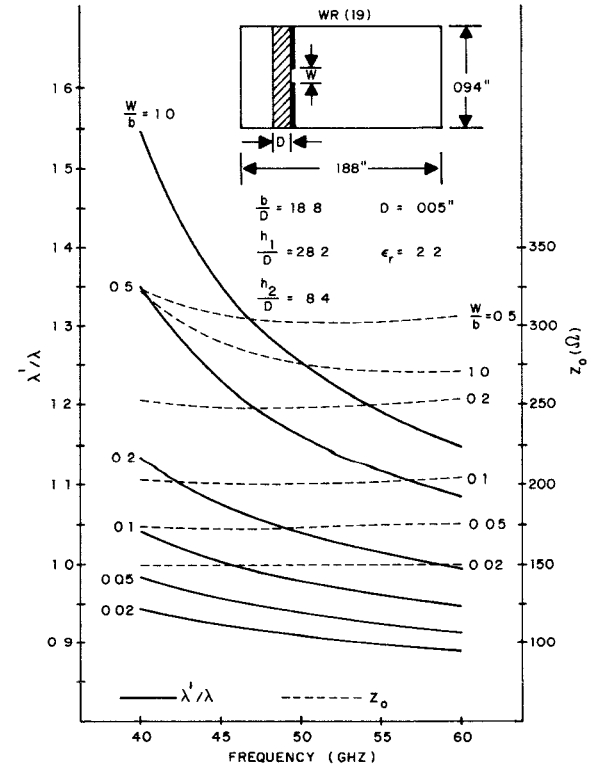

Fig. 11. Wavelength ratio λ'/λ and characteristic impedance Z_0 versus frequency for a fin line with WR(19) shield. Fins are located halfway between side wall and guide center.

dyadic Green's function to be calculated, and circumvents the extensive algebraic manipulation associated with formulations described previously. Numerical results obtained using this method have been presented and compared to other existing data. Good agreement was obtained in all cases thus establishing the accuracy and applicability of the method for the full range of structure parameters. Design curves have been included here for millimeter-wave fin lines of practical interest. Both center and off-center fin locations have been discussed, and the off-center location was shown to result in no significant change in impedance for small values of W/b. Lower impedance may be realized, however, by using a single-fin configuration.

It is clear from the results presented here that the fin line may exhibit the characteristics of a ridged waveguide, slotline, or dielectric slab-loaded waveguide, depending upon the values of the various fin-line parameters. All of these structures are fin-line substructures.

References

[1] P. J. Meier, "Integrated fin-line millimeter components," *IEEE Trans. Microwave Theory Tech.* vol. MTT-22, pp. 1209–1216, Dec. 1974.

[2] ——, "Millimeter integrated circuits suspended in the *E*-plane of rectangular waveguide," *IEEE Trans. Microwave Theory Tech.*, vol. MTT-26, pp. 726–733, Oct. 1978.

[3] ——, "Printed circuit balanced mixer for the 4 and 5 mm bands," in *IEEE MTT-S Symp. Dig.*, pp. 84–86, May 1979.

[4] W. Kpodzo *et al.*, "A quadriphase modulator in fin-line technique," in *IEEE MTT-S Symp. Dig.*, pp. 119–121, May 1979.

[5] A. M. K. Saad and K. Schunemann, "A simple method for analyzing fin-line structures," *IEEE Trans. Microwave Theory Tech.*, vol. MTT-26, pp. 1002–1007, Dec. 1978.

[6] W. Hoefer, "Fin-line parameters calculated with the TLM method," in *IEEE MTT-S Symp. Dig.*, pp. 341–343, May 1979.

[7] T. Itoh, "Spectral domain analysis of dominant and higher order modes in fin-lines," in *IEEE MTT-S Symp. Dig.*, pp. 344–345, May 1979.

[8] T. Itoh and R. Mittra, "Dispersion characteristics of slot lines," *Electron. Lett.*, vol. 7, pp. 364–365, July 1971.

[9] ——, "Spectral-domain approach for calculating the dispersion characteristics of microstrip lines," *IEEE Trans. Microwave Theory Tech.*, (Short Papers), vol. MTT-21, pp. 496–499, July 1973.

[10] ——, "A technique for computing dispersion characteristics of shielded microstrip lines," *IEEE Trans. Microwave Theory Tech.* (Short Papers), vol. MTT-22, pp. 896–898, Oct. 1974.

[11] J. B. Knorr and K -D. Kuchler, "Analysis of coupled slots and coplanar strips on dielectric substrate," *IEEE Trans. Microwave Theory Tech.*, vol. MTT-23, pp. 541–548, July 1975.

[12] J. B. Knorr and A. Tufekcioglu, "Spectral-domain calculation of microstrip characteristic impedance," *IEEE Trans. Microwave Theory Tech.*, vol. MTT-23, pp. 725–728, Sept. 1975.

[13] S. Hopfer, "The design of ridged waveguides," *IRE Trans. Microwave Theory Tech.*, vol. MTT-3, pp. 20–29, Oct. 1955.

[14] R. O. Lagerlöf, "Ridged waveguide for planar microwave circuits," *IEEE Trans. Microwave Theory Tech.*, vol. MTT-21, pp. 499–501, July 1973.

[15] R. Collin, *Field Theory of Guided Waves*. New York: McGraw-Hill, 1960.

[16] P. H. Vartanian *et al.*, "Propagation in dielectric slab loaded rectangular waveguide," *IRE Trans. Microwave Theory Tech.*, vol. MTT-6, pp. 215–222, Apr. 1958.

[17] E. A. Mariani *et al.*, "Slot line characteristics," *IEEE Trans. Microwave Theory Tech.* (1969 Symp. Issue), vol. MTT-17, pp. 1091–1096, Dec. 1969.

The Accuracy of TLM Analysis of Finned Rectangular Waveguides

YI-CHI SHIH, STUDENT MEMBER, IEEE, AND WOLFGANG J. R. HOEFER, SENIOR MEMBER, IEEE

Abstract—**This paper investigates three sources of error affecting the Transmission Line Matrix (TLM) analysis of finned rectangular waveguides. It is shown how truncation and velocity errors can be minimized, and a diagram for maximum coarseness error affecting the TLM analysis is presented. After error correction, cutoff frequencies obtained with the TLM method are in excellent agreement with results obtained with the Transverse Resonance Method.**

Manuscript received September 28, 1979; revised January 24, 1980. This work was supported by the Natural Sciences and Engineering Research Council of Canada under Grant A 7620.

The authors are with the Department of Electrical Engineering, University of Ottawa, Ottawa, Ont., Canada K1N 6N5.

I. Introduction

THE TWO-DIMENSIONAL Transmission Line Matrix (TLM) method was developed by Johns and Beurle [1] and has been successfully applied to waveguide bifurcation scattering problems [1] and to the ridged waveguide problem [2].

It is a powerful tool for solving the homogeneous wave equation in complex structures and, therefore, can be used to verify the accuracy of approximate solutions, provided that the errors affecting the TLM solution are known and can be corrected. The aforementioned authors have

0018-9480/80/0700-0743$00.75 ©1980 IEEE